Automatic estimation of individual tree positions from aerial photos

Kim Dralle and Mats Rudemo

May 13, 1997

Kim Dralle Danish Forest and Landscape Research Institute, Hørsholm Kongevej 11, DK-2970 Hørsholm, Denmark

Mats Rudemo[1] Department of Mathematics and Physics, The Royal Veterinary and Agricultural University, DK-1871 Copenhagen, Denmark

[1] Author to whom all correspondence should be addressed.
Tel: +45 35 28 23 36
Fax: +45 35 28 23 50
E-mail: mats@dina.kvl.dk

ABSTRACT

An automatic method is suggested for estimating the positions of individual trees from panchromatic aerial photos of even-aged homogeneous stands of Norway spruce (*Picea abies* (L.) Karst.). The scanned photo is smoothed by a two-dimensional isotropic Gaussian kernel such that the number of local maxima above the most frequent grey level is approximately equal to the number of trees. The positions of trees at ground level are estimated by use of a displacement model incorporating the angle to the sun, the camera position and estimated tree heights. Parameters of the model are estimated from data for a thinning experiment with six thinning treatments and field measurements of the individual tree positions at ground level. The displacement model is used for matching trees and maxima. It is found that for medium and heavy thinning about 95%, and for light thinning about 85%, of the trees can be detected, and that the root-mean-square residual error in the displacement model is about 65 cm. For estimation of tree positions at ground level additional errors due to uncertainties in the heights may become important, in particular for trees far from the nadir point.

Introduction

"Silvicultural prescriptions and forest management decisions often rely on yield tables that do not model the effects of spacing and thinning regime on either stand or individual tree growth. These shortcomings can severely limit the potential of decision analysis." (Skovsgaard, 1996). Individual tree models — on the other hand — are often capable of taking both the effect of spacing and tree characteristics into account, cf. Daniels and Burkhart (1988) and Penttinen et al. (1992). Individual tree models provide a number of advantages, for instance: (i) enhanced flexibility with regard to stand treatment, (ii) the possibility to incorporate individual tree characteristics such as diameter at breast height, tree height, quality and health status, and (iii) the possibility to model multi-layered mixed forest stands, and to include biodiversity measures. However, a major drawback of these models is the expense associated with field measurements of positions of individual trees (Davis and Johnson, 1987; Vanclay, 1994). Thus distance dependent growth and yield models have not gained attention according to their obvious potential — even though they have a long tradition in research. Särkkä and Tomppo (1996) provide, for example, a list going back to 1974 of references for pairwise interaction models.

A natural question is whether remote sensing can provide data for individual tree models. Unfortunately, the spatial resolution of today's satellite sensors is not sufficient for estimation of individual tree positions. However, airborne sensors such as cameras for aerial photography do provide a potentially high spatial resolution, depending on flight altitude and system resolution. In good weather conditions it is thus possible to obtain a ground projected pixel dimension of 15 cm in a scanned photograph, acquired by a modern wide angle camera at flight altitudes up to 1500 m, when the scanner has a sampling density of at least 1700 dots per inch.

Recently Gougeon (1995) has presented a digital image processing method to single out individual trees by following valleys between maxima corresponding to tree crowns in high spatial resolution multispectral aerial images. He found that, in a plantation scene, 81% of the delineated tree crowns are the same as those obtained by human visual interpretation of the images. In Pollock (1994) an automatic recognition method is suggested for individual trees in aerial images based on a synthetic tree crown model with light reflected both directly from the sun and from the sky. For non-plantation forest scenes success rates of 57% or 74% are achieved, depending on whether all trees or only trees with almost no physical contacts were considered. The method is described in detail in Pollock (1996) including comparisons with human observer success rates and the accuracy of crown diameter estimation.

A method for estimating the stem number in even-aged plantations of Norway spruce (*Picea abies* (L.) Karst.) by kernel smoothing of scanned panchromatic aerial photos was presented in Dralle and Rudemo (1996), and error rates of about 10% was obtained in a small-scale cross-validation study. The possibility of estimating individual tree positions was mentioned, and this problem is addressed here.

There is one crucial parameter that has to be determined in the kernel smoothing method: the bandwidth. It can either be estimated as the intersection between an 'external' and an 'internal' curve as in *op. cit.*, or we can smooth precisely as much as needed to make the total number of maxima equal to the estimated or known number of trees in a given region. For simplicity, we consider here the last mentioned procedure. Starting with this initial procedure we elaborate on the tree position estimation, suggest a model

for systematic and random displacements, estimate the corresponding parameters by use of data where we also have the ground truth, and discuss how these estimates may be utilized in practice when we do not have such ground truth.

Data

The thinning experiment chosen for examination, sample plot KU, constitutes part of an even-aged plantation of Norway spruce located approximately 40 kilometers north-west of Copenhagen. The age of the plantation was 48 years at the time of image acquisition (August 1994), and the average height corresponding to mean basal area was about 22 m. The sample plot is divided into 6 subplots, see Fig. 1, with thinning treatments ranging from no thinning to very heavy thinning, which include those applied to forest stands in practice. Each treatment is represented as both a net and a gross subplot, where the net subplots are surrounded by a belt of trees submitted to the same treatment as the enclosed net subplot. A gross subplot consists of a net subplot and the surrounding belt. The gross subplots are separated by tracks. For a detailed description of the thinning experiment, aerial photography and scanning, see Dralle and Rudemo (1996).

[Fig. 1 about here]

Two photos, 147 and 148, taken at a flight altitude of about 560 m and subsequently scanned to obtain digital images, are analysed in the present paper. Image 148 has its nadir point located within the examined thinning experiment and image 147 has its nadir point located approximately 75 m south of the experiment. The ground projected pixel dimension is approximately 0.15 m for both images. The photos were taken on August 4, 1994 with a Zeiss RMK top 15/23 wide-angle camera with nominal scale 1:4000.

For the present study, the locations, the diameters at breast height, and the heights of some individual trees have also been recorded. The trees were positioned relative to ten control points surrounding the thinning experiment. The position of each tree was estimated by locating a fixed mark at breast height with a Criterion 400 Survey Laser (Liu, 1995). Subsequently this position was shifted to the tree center at ground level by use of the measured diameter (at breast height as all tree diameters referred to in this paper). Approximately every 4 to 6 years since 1970, diameters have been measured for individual trees within the net subplots as averages of two perpendicular measurements. On those occasions corresponding heights and diameters have been registered for approximately 10-15 trees in each net subplot, and the same trees were repeatedly measured. Thus the diameter and height change over time in the net subplots is well known; therefore no further diameter measurements were taken in the net subplots in 1994. Instead the diameters were predicted from the existing data (in which the most recent measurements were taken in spring 1991) by a straight-line regression of diameter on time (Dralle, 1997). The diameters of the trees in the surrounding belts were measured for the first time in 1994. No corresponding heights were measured in the belts. Those previously measured within the net subplots were considered sufficient since the treatment in the belts does not differ from the enclosed subplot.

From the corresponding heights and diameters in 1991, linear regression functions between heights and log diameters were estimated subplot-wise, cf. Henriksen (1950, p. 195). The 1994 heights of the individual trees were then estimated from the actual or updated diameters with the "three years old" regression coefficients (with a resulting standard

deviation of about 1m), see (Dralle, 1997) for details.

Problem specification

Generally, the problem we consider is to specify the connection between, on one hand, the positions and other characteristics of the trees in a stand and, on the other hand, an image obtained from an aerial photo: say, between the white line segments and the grey-level image in Fig. 2.

[Fig. 2 about here]

In this paper we will study a simplified version of this problem. Let $X = \{x_i : i = 1, \ldots, n\}$ denote the tree positions at ground level within an area A of the plane projected onto an image, and let $Y = \{y_j : j = 1, \ldots, m\}$ denote the positions of local maxima of the kernel smoothed image in a corresponding displaced area A_d, obtained by projection onto the image of a suitably elevated plane, where we expect to find the maxima. A model for the displacement from tree position at ground level to the corresponding light maximum is given in Fig. 3, which will be explained in the sections below. We may, for instance, let A be the lower right quadrilateral in Fig. 4 and let X be the set of lower right end-points of line segments within A. Further, we let A_d be the upper left quadrilateral and Y the set of small black squares (diamonds) within A_d.

[Fig. 3 about her]

[Fig. 4 about here]

Elaborating further, we consider how to specify under simplifying assumptions the conditional distribution $P(Y|X)$ for the point process Y in A_d, conditional upon the point process X in A. The following section gives one possible model for which this conditional distribution may be computed.

A model for grey-level maxima given tree positions and heights

The model for the locations of image maxima, given tree positions and heights and sun position, contains three sources of distortion:

(i) some trees are lost (errors of omission),

(ii) the remaining trees become displaced, as a consequence of the image geometry and the lighting conditions; the displacement of a point x_i is composed of a systematic displacement from x_i to x_i' and a random displacement from x_i' to $x_i' + z_i$,

(iii) some spurious maxima that do not correspond to real trees are generated (ghost trees, errors of commission).

In the model we will make the simplifying assumption that these three mechanisms are mutually independent, and further that within each of these three categories the trees behave independently of each other. More specifically, we assume:

(i) For each tree there is a probability θ_0, depending on the thinning treatment, that the tree gives rise to a maximum. Thus the probability of an error of omission is $1 - \theta_0$ for each tree, and the events that different trees are omitted are independent.

(ii) The systematic displacement to x_i', see Fig. 3, of the base location x_i of a tree is obtained by two displacements in the horizontal plane, or, equivalently, in the image plane. Move first along the projection of the tree a distance $\theta_1 p_i$, where p_i is the projection length, and move then orthogonally in the horizontal plane (to the same side of the tree projection as the sun) a distance $\theta_2 h_i \sin\alpha_i$. Here h_i is the height of the tree and α_i is the angle between the horizontal projection of the tree and a line which is the intersection of the horizontal plane and a vertical plane containing both x_i and the sun. The subsequent random motion $z_i = (z_{i1}, z_{i2})$ in the local coordinate system with one axis parallel to the tree projection and one axis orthogonal to it has a two-dimensional normal distribution with means zero, standard deviations σ_1 and σ_2 and correlation coefficient ρ.

(iii) Spurious maxima are generated by a Poisson process with the intensity λ maxima per hectare.

For the systematic displacement from x_i to x_i' and for a maximum $y_{j(i)}$ in the smoothed image corresponding to the base location x_i, we thus have

$$x_i' = x_i + \theta_1 p_i e_{i1} + \theta_2 h_i \sin\alpha_i \, e_{i2} \tag{1}$$

and

$$y_{j(i)} = x_i' + z_i = x_i' + z_{i1} e_{i1} + z_{i2} e_{i2}, \tag{2}$$

where z_{i1} and z_{i2} are random errors and e_{i1} and e_{i2} are unit vectors, see Fig. 3.

To motivate the simple model (1) for the systematic displacement, think of Fig. 3 as the horizontal plane and a tree placed at x_i pointing upwards orthogonally to the paper. For variations in tree position that are small compared to the distance to the camera and for uniformly shaped trees with moderately varying sizes it seems reasonable that the systematic displacement should be proportional to tree size, and further that displacement orthogonal to the projection should behave approximately as the sine function as a function of the angle α_i to the sun: be zero for $\alpha_i = \pi$ in Fig. 3 and then to increase to a maximal value as α_i decreases to $\pi/2$, when the off-axis side of the tree crown becomes directly illuminated.

We assume that the parameters θ_0, θ_1, θ_2, σ_1, σ_2, ρ and λ are constant within subplots. But we will see in the Results section that some of them vary between subplots and images in a way that may be interpreted in terms of thinning treatments and the geometry at image aqcuisition.

Parameter estimation

Methods will be presented here for estimation of the parameter θ_0 for the probability of finding trees, the parameters θ_1 and θ_2 for systematic displacements of base positions, the parameters σ_1, σ_2 and ρ for the additional random displacements, cf. Fig. 3, and the parameter λ for errors of commission.

The parameters are estimated either individually for subplots or for a group of subplots. The estimation procedure is iterative. For trees in a polygonal area A we compute

a displaced area A_d by moving each border polygon corner point according to the transformation (1) as if the border point was the ground location of a tree with a height computed from the height-diameter regression when the tree diameter corresponds to mean basal area of the subplot. Here the current estimates of θ_1 and θ_2 are used.

For a tree with base x_i we compute the position x_i' according to (1) and around this point we let an ellipse with constant probability density according to the model (2) grow. Here the current estimates of σ_1 and σ_2 are used, but $\rho = 0$. Ellipses grow simultanously at the same rate around all points $x_i', i = 1, \ldots, n$, for the trees in the regarded area, or, actually, in a slightly larger area as shown in Fig. 4. As soon as an ellipse starting from x_i' catches a maximum in the smoothed image the growth of that ellipse is stopped. If this maximum has not been catched from another point earlier the maximum (at $y_{j(i)}$) is associated with the ith tree with base location x_i. (If the maximum has already been catched from another tree, no maximum is associated with the ith tree; it is considered lost.)

Let $x_i, i \in I'$, be the set of base locations in A for trees that catch maxima, and let $n' \leq n$ be the number of elements in this set. As an estimate for the probability θ_0 that a tree gives rise to a maximum (one minus the probability of omission), put

$$\hat{\theta}_0 = n'/n. \tag{3}$$

Using Eqs. (1) and (2) estimates for θ_1 and θ_2 are obtained by coordinate-wise linear regression analyses along the e_{i1}- and e_{i2}-axes, respectively, for $i \in I'$. Corresponding estimates for σ_1^2, σ_2^2 and ρ are obtained as the sample variances and the sample correlation for the set of the n' two-dimensional residuals $y_{j(i)} - x_i', i \in I'$.

An estimate for the density of spurious maxima (errors of commission) is

$$\hat{\lambda} = (m - m')/|A|, \tag{4}$$

where m is the number of maxima in A_d, and $m' = n'$ is the number of maxima in A_d that are caught by trees and $|A|$ denotes the area in hectares of A.

Initial values for the parameters θ_1 and θ_2 are needed in the iterative estimation for determining the elevated plane mentioned in the "Problem specification" section: this plane is used to obtain the relevant set of maxima. The initial values turn out not to be critical and they may, for instance, be chosen from results of previous analyses of other similar data sets, cf. Table 1 below. The estimation procedure is iterated until no further changes in the parameter estimates are obtained.

Results

For both images, the subplots D, C, R, DB and B are analysed individually and in groups: 'all except B' and 'all'. The reason for excluding B in the first group analysis is that B has a consistently lower θ_0-estimate compared to the other treatments. The resulting parameter estimates are all listed in Table 1, and the result for image 148 and treatment D is shown in Fig. 4.

The root-mean-square random displacement in metres is

$$\sigma = 0.15\,(\sigma_1^2 + \sigma_2^2)^{1/2}, \tag{5}$$

and it is also given in Table 1.

In Fig. 5 the estimates of the parameters θ_0, θ_1, θ_2 and λ are plotted against the true stem number N, and in Fig. 6 the two-dimensional residual errors $(\hat{z}_{i1}, \hat{z}_{i2})$ are shown.

[Table 1 about here]

[Fig. 5 about here]

[Fig. 6 about here]

Discussion

The method for estimation of individual tree positions presented in this paper gives acceptable results for the two images studied. For medium and heavy thinning, around 95% (the parameter θ_0 in Table 1) of the trees are found with a root-mean-square residual error in the displacement model of about 65 cm, and for light thinning around 85% of the trees are found and positioned with comparable precision. The unthinned control was not investigated here because this treatment gives an exceptionally dense population, and a large number of trees are suppressed, which means they cannot be seen from the air, cf. Dralle and Rudemo (1996).

The simple model for errors of omission and commission and for systematic and random displacements seems useful, although it could certainly be refined. Thus the arrows in Fig. 4, pointing at spurious maxima, indicate that maxima associated with small "watershed" segments have a higher probability of being spurious than maxima associated with large segments. Similarly, a close look at the omitted trees indicates that omissions may be caused by large trees which (partly) occlude smaller trees.

One could try to use the maximum likelihood method corresponding to our statistical model (1) – (2) for the present data set with both the image and the ground truth available. However, a computation that takes all possible correspondences between the set of maxima and the set of trees is prohibitive, as the number of such correspondences is astronomical. One possibility, which is currently being investigated, is to consider a small subset of the most "probable" correspondences. In the present paper we have been even more reductionistic, considering only one such correspondence specified in the two paragraphs preceding Equ. (3). After establishing the correspondence, the subsequent parameter estimation is straightforward, particularly if we assume that the correlation between errors along the tree projection and orthogonal to it is zero, as we have done in the present paper. Then θ_1 and σ_1 are estimated by use of the differencies along the tree projections, and θ_2 and σ_2 are estimated from the differences in the orthogonal direction. A minor complication is that the set of maxima that we regard for a given subplot depends slightly on the the estimates of θ_1 and θ_2, and thus we have chosen to iterate the procedure until no further changes were obtained. Only a small number of iterations were needed.

From Fig. 5 we see that the probability of omission, $1 - \theta_0$, and the expected number λ of errors of commission per hectare both increase with stem number. It may be noted that due to our method of determining the kernel bandwidth so that the number of trees within each subplot is approximately correct, the errors of omission and the errors commission tend to vary together. But is seems reasonable to conjecture that also with other methods of tuning the bandwidth, these errors will both increase in number with the stem number.

The parameter θ_1 of the displacement model varies between images and with the thinning treatment, see Fig. 5. It is larger for image 147 than for image 148, presumably due

to increased occlusion among trees with increased distance to the nadir point. Note that the location of a maximum in the appropriately smoothed image is typically an average location of a tree's sun-lit parts visible from the camera position. Similarly, the increase of θ_1 with the stem number could be due to increased occlusion among trees with increasing stem number. Note that although the tree heights decrease with increasing stem number the ensuing decrease in distance between nearest neighbours is much more pronounced. With increased stem number we also get increased shading among trees, which similarly may cause an increase of θ_1. The row thinning (R), where every second row has been removed at an early stage, behaves differently compared to the other treatments. That may originate from the systematic row-pattern with special light conditions.

The variation of θ_1 with thinning may partly also be due to change in tree shape. The crown ratio, or crown height, is known to change with stand height (stand age) and stand density, see for example Assmann (1970). With increasing stand height, crown ratios tend to decrease, and with increasing stand density, crown ratios also tend to decrease. In the present study, where the age is fixed, the variation of stand height is mainly a treatment effect, i.e., caused by successive thinning of the smallest trees. Particularly in the heavy thinned treatment the large and fast growing trees are favoured. Monserud and Sterba (1996) showed that faster growing trees have higher crown ratios than slow growing trees. Thus if we consider individual trees not shaded or occluded by neighbours the crown ratio in conjunction with sun altitude determine how high up along the stem the intensity peak in the smoothed image can be expected. The more dense the stand, the higher up the peak is expected.

A subjective evaluation of the residual plots in Fig. 6 indicates that the two-dimensional normal model for the random displacements errors seems satisfactory. From Fig. 6 and also from Table 1 we see that the component of random displacement along the projection of the tree (along the x-axes in Fig. 6 and also measured by σ_1) is larger than the orthogonal component (along the y-axes and also measured by σ_2) for subplots C, R, DB and B, but not for subplot D. That subplot D is exceptional in this respect is quite natural as the trees in D have comparatively broad crowns due to sufficient space for the individual trees. We note also that the root-mean-square random displacement estimate $\hat{\sigma}$ in Table 1 is larger for subplot D than for subplots C, R and DB.

In the analysis of the present paper we have looked at the displacement from a tree base position x to a maximum located at y in the smoothed image. In practice, we typically have only the position y of a maximum and want to estimate the base position x of a corresponding tree. Comparing with Equ. (1) and Fig. 3 we suggest the use of the estimator

$$\hat{x} = y - \theta_1 p\, e_1 - \theta_2 h \sin\alpha\, e_2. \tag{6}$$

Here e_1 and e_2 are orthogonal unit vectors, h is the height of the tree, p is the corresponding projection length, α an angle, (cf. Fig. 3), while θ_1 and θ_2 are parameters. All these quantities need to be estimated. Although the unit vectors should properly be located relative to x, it will typically be sufficient to let e_1 point in the direction away from nadir through y, to let e_2 be orthogonal to e_1 and to be directed to the same side of e_1 as the sun, and, similarly, to let the angle α be measured at y instead of x. The height of the tree could be estimated from the age of the stand by use of a local growth table, and the projection length may be estimated from the estimated camera position. In Danish practice this height is a fairly accurate measure of the stand height, and the

height variation among trees is small. Thus for images obtained under similar geometric conditions as images 147 and 148, we suggest that the parameter estimates in Table 1, see also Fig. 5, for θ_1 and θ_2 could be used. Similarly we could use the other estimates in Table 1: the estimates of θ_0 and λ to estimate the probabilities of errors of omission and commission, and the σ_1-, σ_2- and σ-estimates to estimate the size of the random residual position error.

What is the error in positioning if we use the estimator (6) with estimated quantities h, p, θ_1 and θ_2? One component is the random residual error, that is, z_i in Equ. (2), but in addition we have errors in the estimated quantities. For estimation of the global position error, the estimate of θ_1 may be dominating, although this estimate seems rather stable, cf. Fig. 5. For estimation of local properties, such as the distance to nearest neighbours in, say, even-aged stands with medium or heavy thinning it may well be that the residual random errors together with the error in the estimated height are most important sources of error. The influence of the error in the estimated height is comparatively small close to the nadir point.

Let us give a rough estimate of the angle at which the standard error due to height variability is equal to the standard error from the displacement model, i.e. about 65 cm. Consider a plantation with mean height 20 meters and a height standard deviation of 1 m, which may be realistic under Danish conditions. The corresponding angle is $\arctan 0.65 = 33$ deg. For stands with a large height standard deviation, the critical angle is evidently much smaller.

Thus, for trees not close to nadir, it seems necessary to use multiple views and stereo methods to obtain accurate locations at ground level. In addition, stereo methods will then simultaneously give estimates of tree heights. These questions are presently being investigated.

Conclusions

For estimating the position of a tree at ground level we suggest the estimator (6), which is based on the displacement model (1) – (2). By use of two images for which we also have the ground truth, the parameters are estimated and the properties of the model are evaluated. For images with the nadir point close to the stand under study the method seems to function well. It is found that for medium and heavy thinning about 95%, and for light thinning about 85%, of the trees can be detected. The root-mean-square residual error in the displacement model is about 65 cm. For accurate determination of tree positions not close to the nadir point, in particular, if we use a wide-angle camera, it seems necessary to either have good estimates tree heights, or to use multiple views and stereo modelling. For the use of stereo methods, the model of the present paper may give a useful starting point.

Acknowledgements

The research reported in this paper was supported by the Danish Agricultural and Veterinary Research Council through Dina, Danish Informatics Network in the Agricultural Sciences, and by the National Forest and Nature Agency of Denmark. We are further

indebted to Morten Larsen for providing a program for finding maxima and to the referees for a number of valuable comments.

References

Assmann, E. (1970). *The Principles of Forest Yield Study.* Pergamon Press, Oxford.

Daniels, R. F. and Burkhart, H. E. (1988). An integrated system of forest stand models. *Forest Ecology and Management*, 23 (1988):159–177.

Davis, L. S. and Johnson, K. N. (1987). *Forest Management.* McGraw-Hill, Inc., New York.

Dralle, K. (1997). *Locating trees by image processing of digital aerial photos.* PhD thesis, Danish Forest and Landscape Research Institute and Dep. Mathematics, the Royal Veterinary and Agricultural University. March, 1997.

Dralle, K. and Rudemo, M. (1996). Stem number estimation by kernel smoothing in aerial photos. *Canadian Journal of Forest Research.* 26: 1228-1236.

Gougeon, F. A. (1995). A crown-following approach to the automatic delineation of individual tree crowns in high spatial resolution aerial images. *Canadian Journal of Remote Sensing*, 21(3):274–284.

Henriksen, H. A. (1950). Height-diameter diagram with logarithmic diameter (in Danish). *Dansk Skovforenings Tidsskrift*, 35:193–202.

Liu, C. J. (1995). Using portable laser EDM for forest traverse surveys. *Canadian Journal of Forest Research*, 25:753–766.

Monserud, R. A. and Sterba, H. (1996). A basal area increment model for individual trees growing in even- and uneven-aged forest stands in Austria. In *Forest Ecology and Management*, 80:57–80.

Penttinen, A., Stoyan, D., and Henttonen, H. M. (1992). Marked point processes in forest statistics. *Forest Science*, 38(4):806–824.

Pollock, R.J. (1994). A model-based approach to automatically locating tree crowns in high spatial resolution images. In Desachy, J., editor, *Image and Signal Processing for Remote Sensing*, Proc. SPIE 2315, pages 526-537, Rome, Italy

Pollock, R.J. (1996). *The Automatic Recognition of Individual Trees In Aerial Images of Forests based on a Synthetic Tree Crown Image Model.* PhD thesis, Computer Science, The University of British Columbia, Vancouver, Canada.

Särkkä, A. and Tomppo, E. (1996). Modelling interactions between trees by means of field observations. In *New Thrusts in Forest Inventory*, pages 161–170. EFI Proceedings No. 7, Joensuu.

Skovsgaard, J. P. (1996). Developing a variable-density growth model based on a normal yield table for Norway spruce on former Atlantic heathland in Denmark. *Forest and Landscape Research*, 1:255–274.

Vanclay, J. K. (1994). *Modelling Forest Growth and Yield: Applications to Mixed Tropical Forests.* CABI, Wallingford.

Tables and figures

Table 1: Parameter estimates for the net subplots in images 147 and 148 and five thinning treatments.

Subplot	N	$\hat{\theta}_0$	$\hat{\theta}_1$	$\hat{\theta}_2$	$\hat{\sigma}_1$	$\hat{\sigma}_2$	$\hat{\rho}$	$\hat{\lambda}$	$\hat{\sigma}$
Image number:	147.								
D	367	0.920	0.750	-0.053	3.38	3.43	-0.147	18	0.72
C	625	0.959	0.821	0.057	2.77	1.75	0.065	26	0.49
R	746	0.960	0.806	0.041	3.12	1.69	-0.180	25	0.53
DB	824	0.930	0.844	0.037	3.22	1.85	-0.005	94	0.56
B	1257	0.852	0.870	-0.003	3.12	2.45	-0.268	164	0.60
All except B		0.946	0.818	0.042	3.56	2.30	-0.141	34	0.64
All		0.910	0.822	0.012	3.43	2.62	-0.116	65	0.65
Image number:	148.								
D	367	0.970	0.651	0.028	2.74	2.94	0.370	15	0.60
C	625	0.971	0.731	0.056	2.48	1.69	0.088	37	0.45
R	746	0.980	0.634	0.082	3.20	2.12	-0.313	15	0.58
DB	824	0.956	0.767	0.006	2.69	2.19	-0.219	40	0.52
B	1257	0.843	0.871	0.045	4.29	2.65	-0.035	168	0.76
All except B		0.969	0.730	0.046	3.23	2.76	-0.096	26	0.64
All		0.925	0.734	0.045	3.61	2.75	-0.071	55	0.68

Note: N is the true stem number per hectare; θ_0 is the probability that a tree gives rise to a maximum (and $\hat{\theta}_0$ the corresponding parameter estimate) ; θ_1 and θ_2 specify the systematic displacement from the base location x_i to x_i' at which the corresponding intensity peak is expected (Fig. 3); σ_1, σ_2 (in pixel units corresponding to 15 cm at ground level) and ρ are parameters in a two-dimensional normal distribution for the random displacement z_i from the expected to the observed location (Fig. 3); λ is the expected number of spurious maxima per hectare; σ is the root-mean-square random displacement in metres.

Fig. 1. Thinning experiment KU of 48 year old Norway spruce located approximately 40 kilometers north-west of Copenhagen. The net subplots are shown with their thinning grades, A: no thinning, B: light thinning. C: medium-heavy thinning, D: very heavy thinning, D→B: in youth very heavy, later light thinning, R: heavy row thinning. The nadir points for images 147 and 148 are also marked.

Fig. 2. The image 148 with tree projections superimposed, as seen from the camera position. The tree projections were computed from the tree location field measurements and the tree heights, estimated from height-diameter regression and diameter field measurements, see the text for further details. Of the ten control points surrounding the thinning experiment three points are visible in the figure (north, north-west and west, respectively, of the experiment).

Fig. 3. Displacement model for the positioning of trees. The full-drawn thick line represents the ith tree stem projected, as seen from the camera, onto the image with the base position x_i nearest to the nadir point. The length (in pixel units) of the projection is denoted p_i, and the height of the tree (also in pixel units) is h_i. The systematic displacement takes x_i to the expected position x_i' for the grey-level maximum and an additional random displacement gives the observed location $x_i' + z_i$ of a corresponding maximum. The coordinates of z_i have a two-dimensional normal distribution with zero means.

Fig. 4. Subplot D in image 148 with the net subplot borders (lower right quadrilateral) and the corresponding displaced area where maxima are expected (upper left quadrilateral). The local maxima after smoothing with the optimal bandwidth are shown as small black squares (diamonds), and for each local maximum the corresponding "watershed" segment above median grey level is shown in light grey colour with borders between segments in slightly darker grey colour. Tree projections, as seen from the camera, based on ground measurements are shown as line segments and expected positions for local maxima according to the model indicated in Fig. 3 as stars. From each star an ellipse is grown until it hits a local maximum. The ellipse is dashed if this maximum has already been hit by a smaller ellipse from another star. Thus stars with a dashed ellipse represent errors of omission, while small squares not hit by an ellipse (these squares have pointers to them) represent errors of commission. The sun azimuth is marked in the upper right corner of the image.

Fig. 5. Parameter estimates for θ_0, θ_1, θ_2 and λ plotted against the true stem number per hectare for different subplots: $+$ denote observations in image 147, and $\circ$ denote observations in image 148.

Fig. 6. Two-dimensional residual plots for model check for the two images and five thinning treatments. The residuals are plotted in pixel units, $\hat{z}_{i1}$ along the x-axes, and $\hat{z}_{i2}$ along the y-axes.

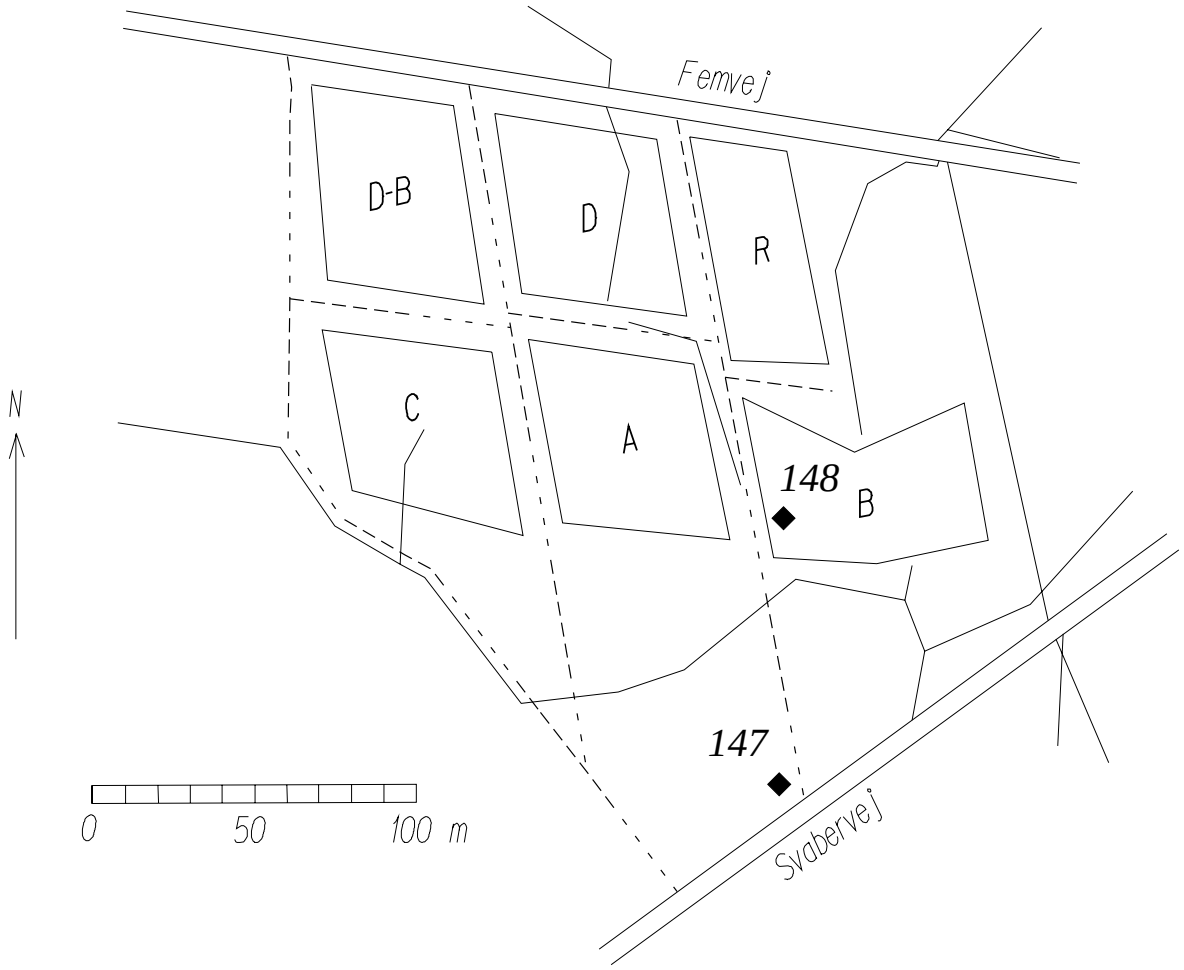

Figure 1

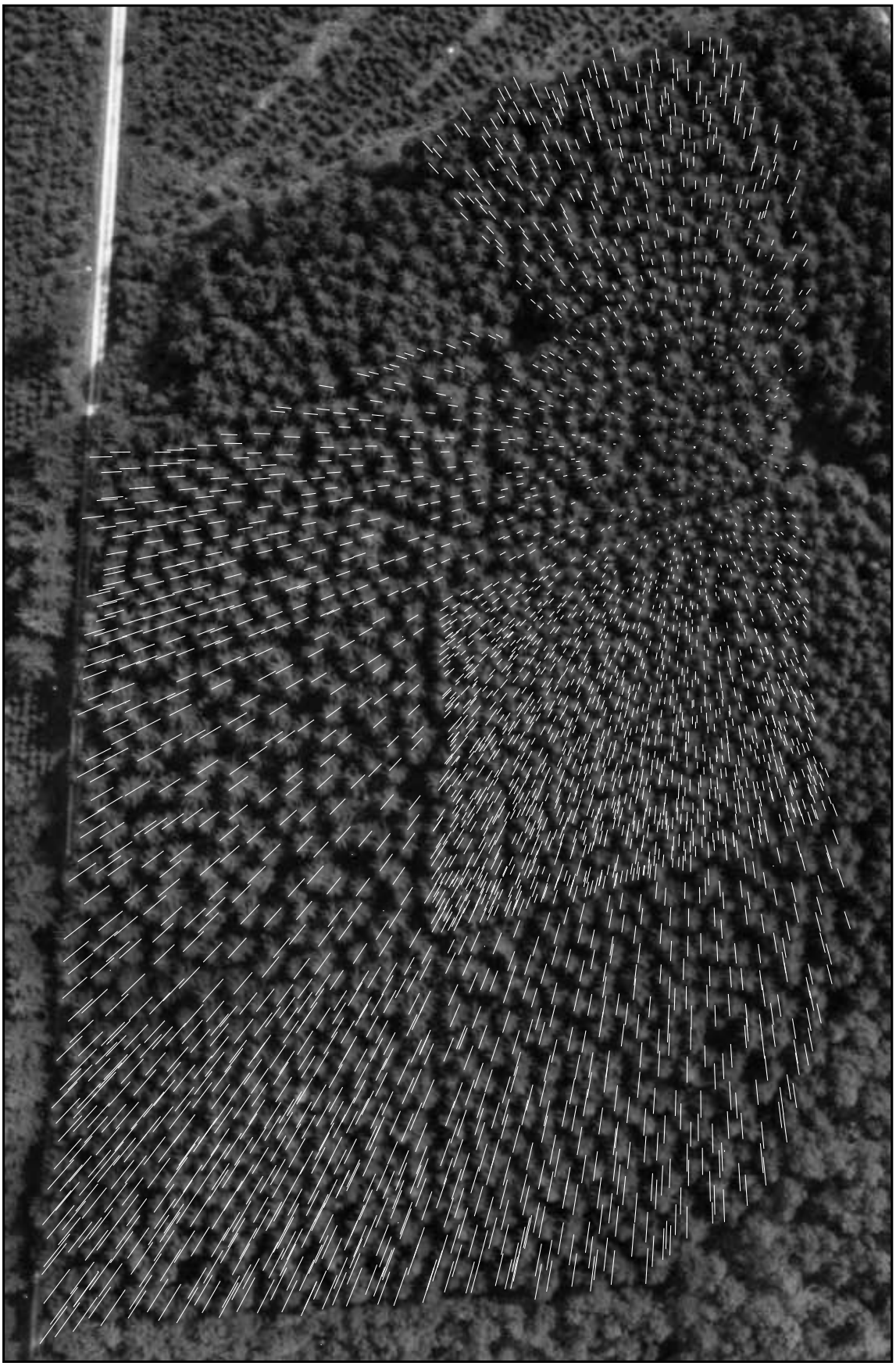

Figure 2

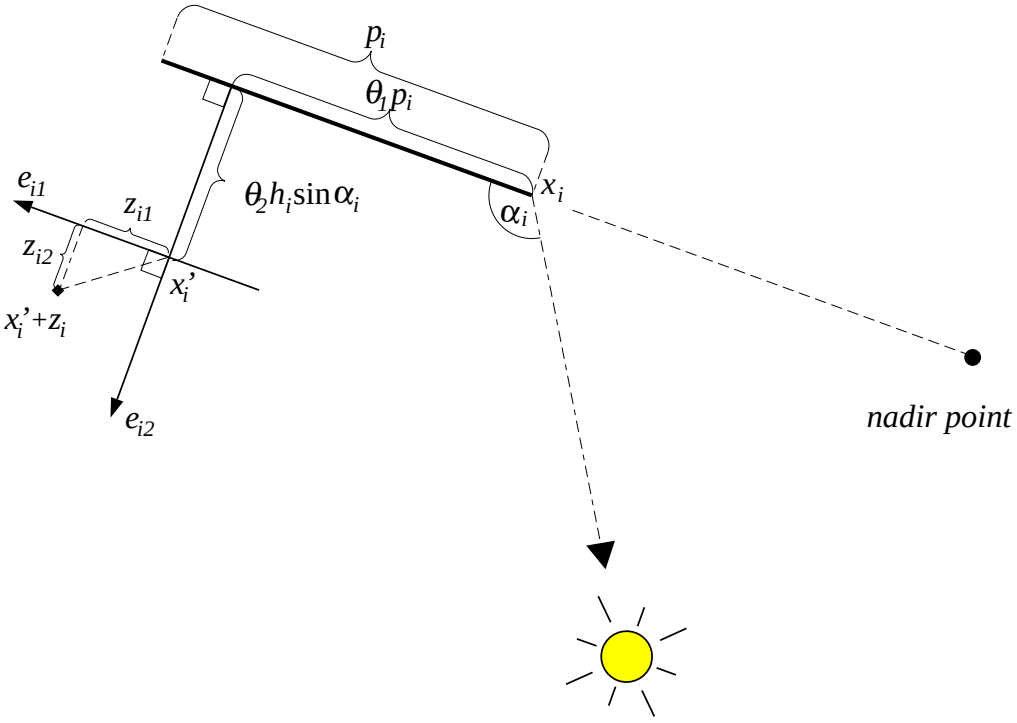
p_i
$\theta_1 p_i$
$\theta_2 h_i \sin\alpha_i$
x_i
α_i
e_{i1}
z_{i1}
z_{i2}
x_i'
$x_i'+z_i$
e_{i2}
nadir point

Figure 3

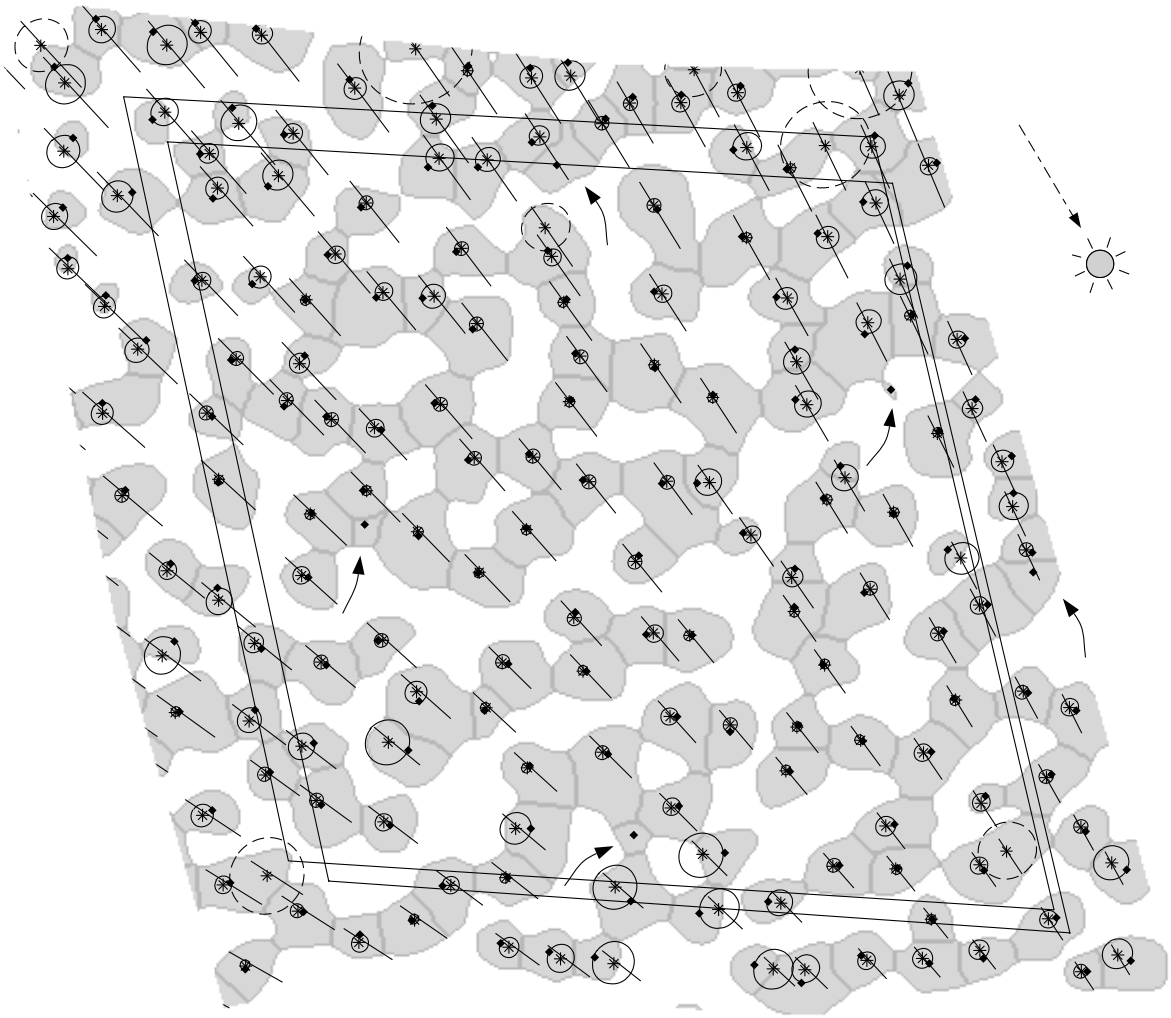

Figure 4

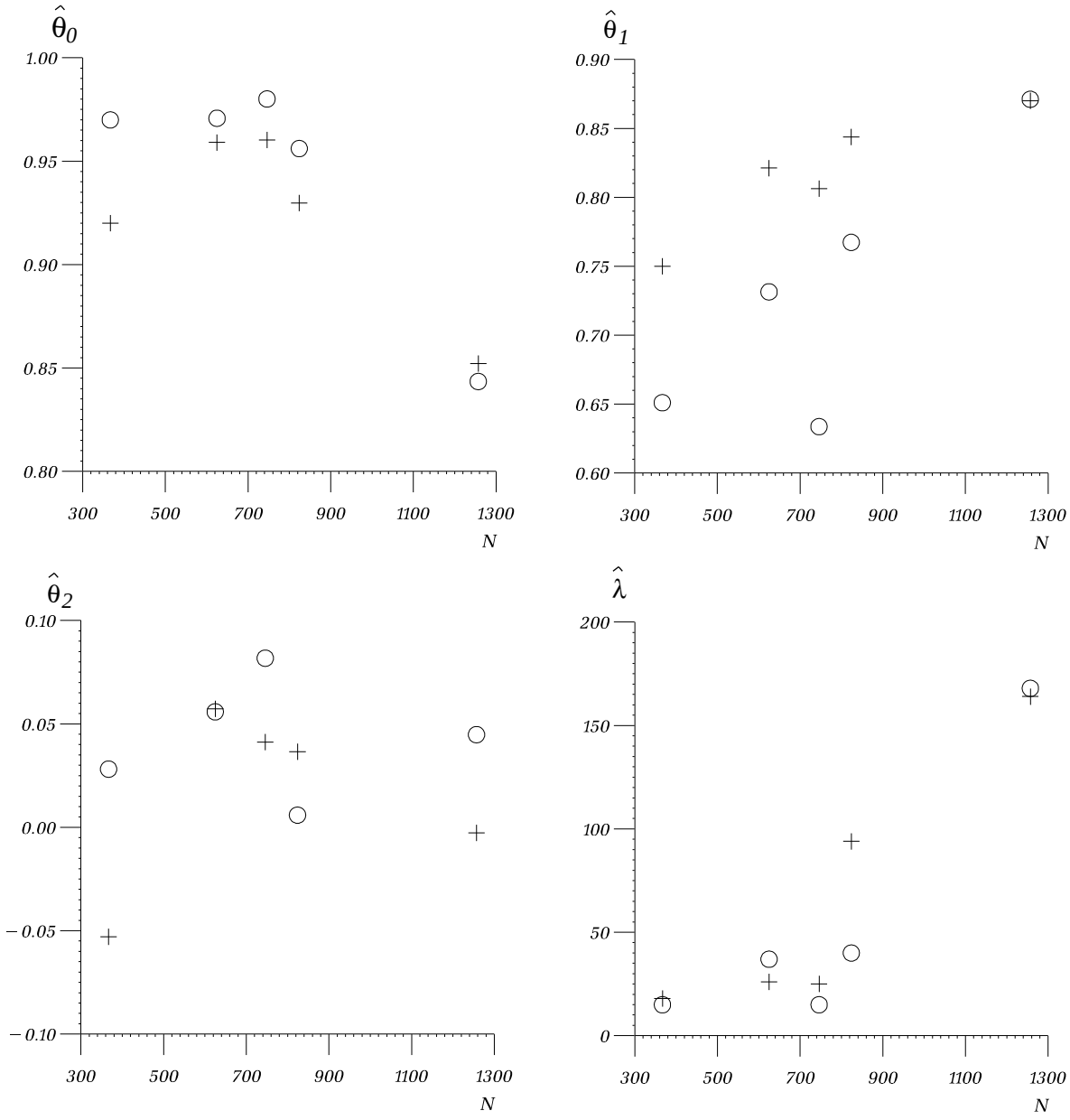
$\hat{\theta}_0$
1.00
0.95
0.90
0.85
0.80
300
500
700
900
1100
1300
N
$\hat{\theta}_1$
0.90
0.85
0.80
0.75
0.70
0.65
0.60
300
500
700
900
1100
1300
N
$\hat{\theta}_2$
0.10
0.05
0.00
− 0.05
− 0.10
300
500
700
900
1100
1300
N
$\hat{\lambda}$
200
150
100
50
0
300
500
700
900
1100
1300
N

Figure 5

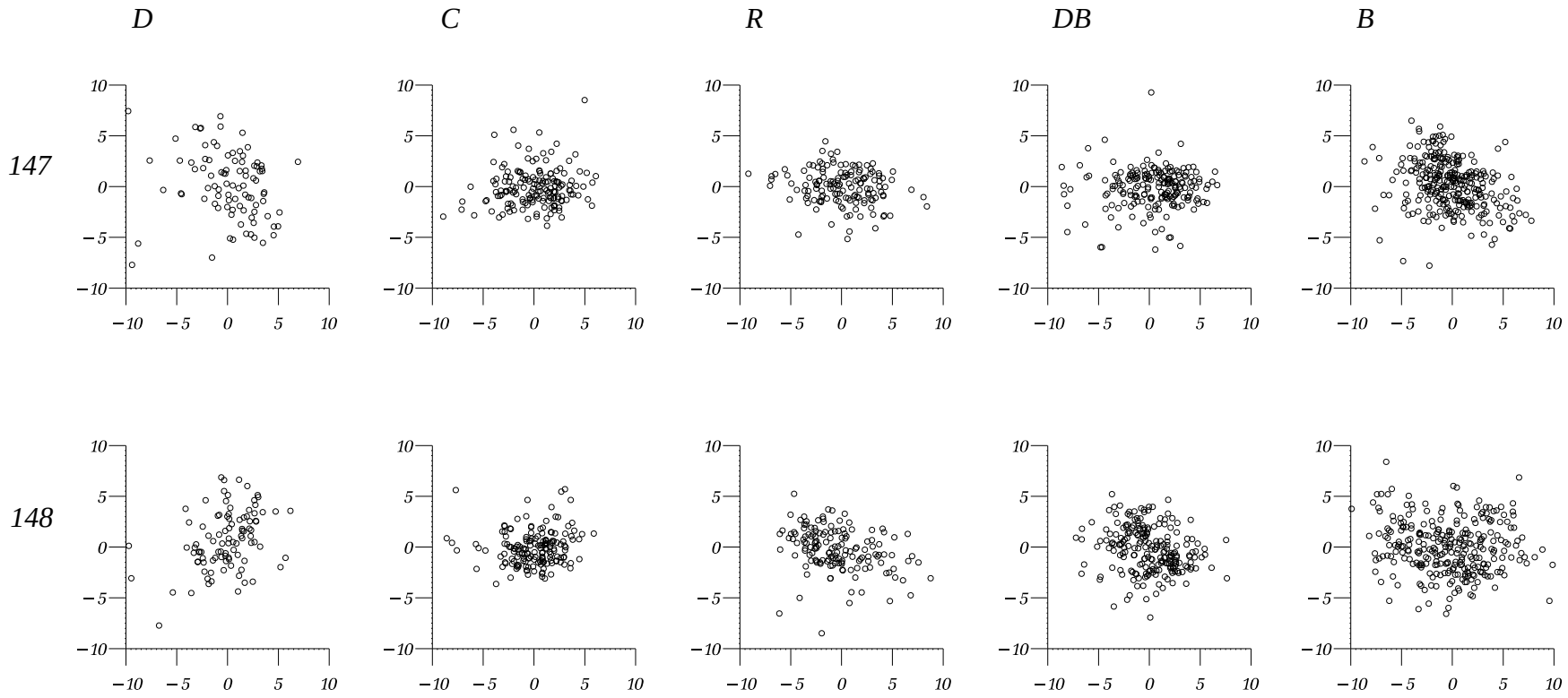

Figure 6